

# Incorporation of cholesterol in sphingomyelin-phosphatidylcholine vesicles has profound effects on detergent-induced phase transitions

Antonio Moschetta,<sup>\*,†</sup> Peter M. Frederik,<sup>§</sup> Piero Portincasa,<sup>†</sup> Gerard P. vanBerge-Henegouwen,<sup>\*</sup> and Karel J. van Erpecum<sup>1,\*</sup>

Gastrointestinal Research Unit,<sup>\*</sup> Departments of Gastroenterology and Surgery, University Medical Center, Utrecht; Section of Internal Medicine,<sup>†</sup> Department of Internal and Public Medicine, University Hospital, Bari, Italy; and Department of Electron Microscopy,<sup>§</sup> Maastricht University, The Netherlands

**Abstract** Vesicle ↔ micelle transitions are important phenomena during bile formation and intestinal lipid processing. The hepatocyte canalicular membrane outer leaflet contains appreciable amounts of phosphatidylcholine (PC) and sphingomyelin (SM), and both phospholipids are found in the human diet. Dietary SM enrichment inhibits intestinal cholesterol absorption. We therefore studied detergent-induced vesicle → micelle transitions in SM-PC vesicles. Phase transitions were evaluated by spectrophotometry and cryotransmission electron microscopy (cryo-TEM) after addition of taurocholate (3–7 mM) to SM-PC vesicles (4 mM phospholipid, SM/PC 40%/60%, without or with 1.6 mM cholesterol). After addition of excess (5–7 mM) taurocholate, SM-PC vesicles were more sensitive to micellization than PC vesicles. As shown by sequential cryo-TEM, addition of equimolar (4 mM) taurocholate to SM-PC vesicles induced formation of open vesicles, then (at the absorbance peak) fusion of bilayer fragments into large open structures (around 200 nm diameter) coexisting with some multilamellar or fused vesicles and thread-like micelles and, finally, transformation into an uniform picture with long thread-like micelles. Incorporation of cholesterol in the SM/PC bilayer changed initial vesicular shape from spherical into ellipsoid and profoundly increased detergent resistance. Disk-like micelles and multilamellar vesicles, and then extremely large vesicular structures, were observed by sequential cryo-TEM under these circumstances, with persistently increased absorbance values by spectrophotometry. These findings may be relevant for bile formation and intestinal lipid processing. Inhibition of intestinal cholesterol absorption by dietary SM enrichment may relate to high resistance against bile salt-induced micellization of intestinal lipids in presence of the sphingolipid.—Moschetta, A., P. M. Frederik, P. Portincasa, G. P. vanBerge-Henegouwen, and K. J. van Erpecum. Incorporation of cholesterol in sphingomyelin-phosphati-

dycholine vesicles has profound effects on detergent-induced phase transitions. *J. Lipid Res.* 2002. 43: 1046–1053.

**Supplementary key words** micelles • spectrophotometry • taurocholate

Micelle ↔ vesicle phase transitions have been studied extensively during the past decades for various reasons. For example, to incorporate membrane proteins into phospholipid vesicles, in general, mixed micelles containing surfactant, phospholipid and the protein of choice are first constructed, and functional insertion of the protein within the bilayer of the vesicles is subsequently obtained by inducing micelle → vesicle transitions through removal of the surfactant. Also, several phase transitions occur during the process of bile secretion. Nascent bile within the canaliculus is generally believed to contain cholesterol-phospholipid vesicles (1). Upon progressive bile concentration in the bile ducts and in the gallbladder, these vesicles are largely transformed into mixed bile salt-phospholipid-cholesterol micelles. During this process, cholesterol crystal formation (an essential step in gallstone formation) may occur in case of cholesterol supersaturated bile, possibly after aggregation of small unilamellar vesicles (2). Alternatively, primordial and multilamellar vesicles have been visualized by cryotransmission electron microscopy during the crystallization process (3–5).

After a meal, the gallbladder empties, and dilution of bile upon entering the intestine induces micelle → vesicle phase transitions. Enzymes within the intestinal lumen such as phospholipase A<sub>2</sub> may then induce the reverse process again with formation of open vesicles, bilayer frag-

Abbreviations: cryo-TEM, cryo-transmission electron microscopy; PC, phosphatidylcholine; SM, sphingomyelin.

<sup>1</sup> To whom correspondence should be addressed.

e-mail: k.j.vanerpecum@azu.nl

Manuscript received 4 October 2001 and in revised form 26 March 2002.

DOI 10.1194/jlr.M100355.JLR200

ments, and micelles (6). The intermediate structures formed during vesicle → micelle transition, and the vesicles and micelles themselves, are thought to be important for optimal activities of various digestive enzymes, and for intestinal absorption of various lipids.

Vesicle ↔ micelle transitions have been studied in some detail by turbidity measurements (7, 8), nuclear magnetic resonance (8, 9), and cryotransmission electron microscopy (10, 11). These studies were generally performed with phosphatidylcholine (PC) as the phospholipid [often with PC from egg yolk, which contains 16:0 acyl chains at the *sn*-1 position and mainly unsaturated (18:1 > 18:2 > 20:4) acyl chains at the *sn*-2 position]. PC is the exclusive (>95%) phospholipid in human bile (with an acyl chain composition similar to egg yolk PC) (12). In contrast, both PC and sphingomyelin (SM) are the major phospholipids of the hepatocyte canalicular membrane outer leaflet (13). Cholesterol has a high affinity for SM (14–16) and is thought to be preferentially located together with this phospholipid in detergent-resistant rafts in the canalicular membrane (17).

Furthermore, considerable amounts of saturated PCs and SMs may occur in human food (18). Recent data in the mouse and rat suggest that dietary SMs, which are relatively resistant to intestinal hydrolysis by alkaline sphingomyelinase (19, 20), may markedly reduce intestinal cholesterol absorption (20, 21). Within the gut lumen, exogenous dietary cholesterol is initially emulsified with other undigested lipids in oily vesicular droplets. The partitioning of cholesterol into bile salt-phospholipid micelles is considered necessary for intestinal cholesterol absorption. The micellar cholesterol then crosses the unstirred water layer followed by the movement of monomeric cholesterol across the brush border membrane either through passive diffusion or by a carrier mediated mechanism (22).

In the present study we examined effects of including SM within egg yolk PC containing-vesicles (with and without cholesterol) on vesicle → micelle phase transitions by means of spectrophotometry and by sequential state-of-the-art cryotransmission electron microscopy. Whereas previous electron microscopy studies were often prone to artifacts such as evaporation, advances in technology now avoid these caveats with the aid of temperature- and humidity-controlled conditions (37°C, 100% humidity, see Materials and Methods).

## MATERIALS AND METHODS

### Materials

Taurocholate was obtained from Sigma Chemical Co. (St. Louis, MO) and yielded a single spot upon TLC (butanol-acetic acid-water, 10:1:1, v/v/v, application of 200 μg bile salt). Cholesterol (Sigma) was ≥98% pure by reverse-phase HPLC (isopropanol-acetonitril, 1:1, v/v, detection at 210 nm). PC from egg-yolk (Sigma), and SM from egg-yolk (Avanti Polar-Lipids Inc., Alabaster, AL) yielded a single spot on TLC (chloroform-methanol-water, 65:25:4, v/v/v, application of 200 μg lipid). Acyl chain compositions as determined by gas-liquid chromatography (23) showed a preponderance of 16:0 acyl chains for egg yolk SM. As

shown by reverse-phase HPLC, egg yolk PC contained mainly 16:0 acyl chains at the *sn*-1 position and mainly unsaturated (18:1 > 18:2 > 20:4) acyl chains at the *sn*-2 position, similar to phosphatidylcholine in human bile (12). All other chemicals and solvents were of ACS or reagent grade quality.

The enzymatic cholesterol assay kit was obtained from Boehringer (Mannheim, Germany), 3α-hydroxysteroid dehydrogenase for the enzymatic measurement of bile salt concentrations (24) from Sigma. The reverse-phase C18 HPLC column was from Supelco (Supelcosil LC-18-DB, Supelco, Bellefonte, PA).

### Preparation of model systems

Lipid mixtures containing variable proportions of cholesterol, phospholipids (both from stock solutions in chloroform), or taurocholate (from stock solutions in methanol) were vortex-mixed and dried at 45°C under a mild stream of nitrogen and subsequently lyophilized during 24 h before being dissolved in aqueous 0.15 M NaCl plus 3 mM NaN<sub>3</sub>. Tubes were sealed with teflon-lined screw caps under a blanket of nitrogen to prevent lipid oxidation, and vortex-mixed for 5 min followed by incubation at 37°C in the dark. The final mole percentages cholesterol, phospholipids, and bile salt did not differ more than 1% from the intended mole percentages.

### Lipid analysis

Phospholipid concentrations in model systems were assayed by determining inorganic phosphate according to Rouser (25). Cholesterol concentrations were determined with an enzymatic assay (26), and bile salts with the 3α-hydroxysteroid dehydrogenase method (24).

### Preparation of small unilamellar vesicles

Small unilamellar vesicles were prepared by sonication. Lipids, from stock-solutions in chloroform, were vortex-mixed, dried under a mild stream of nitrogen, and subsequently lyophilized during 24 h. The lipid film was dissolved in nitrogen-flushed aqueous 0.15 M NaCl plus 3 mM NaN<sub>3</sub>, and thereafter the suspensions were probe-sonicated during 30 min at 50°C (above the main transition temperatures of the phospholipids). After sonication, the suspension was centrifuged during 30 min at 50,000 *g* at 40°C in order to remove potential remaining vesicular aggregates and titanium particles. The resulting small unilamellar vesicles were stored at temperatures above 40°C and used within 24 h. Small unilamellar vesicles were prepared with 100% PC, or SM 40%/PC 60% as the phospholipid. Final phospholipid concentration was 4 mM. Vesicles were either prepared without or with cholesterol (cholesterol-phospholipid ratio 0 or 0.4).

### Interactions of small unilamellar vesicles with taurocholate

Interactions of small unilamellar vesicles with various taurocholate solutions (final concentrations varying between 3 and 7 mM) were followed by measuring optical density (OD) at 405 nm every minute during 80 min at 37°C in a thermostated Benchmark microplate reader (BioRad, Hercules, CA). The solutions were stirred for 3 s prior to each measurement. During this period, the time course of various phase transitions was visualized by performing cryotransmission electron microscopy at several time points during the incubation. In the case of cholesterol-containing vesicles, at the end of the incubation, the mixtures were also examined by polarizing light microscopy in order to examine whether liquid or solid cholesterol crystals had formed.

*Cryotransmission electron microscopy.* Sample preparation for cryotransmission electron microscopy (cryo-TEM) was done in a temperature and humidity controlled chamber using a fully automated (pc-controlled) vitrification robot (Vitrobot, patent applied).

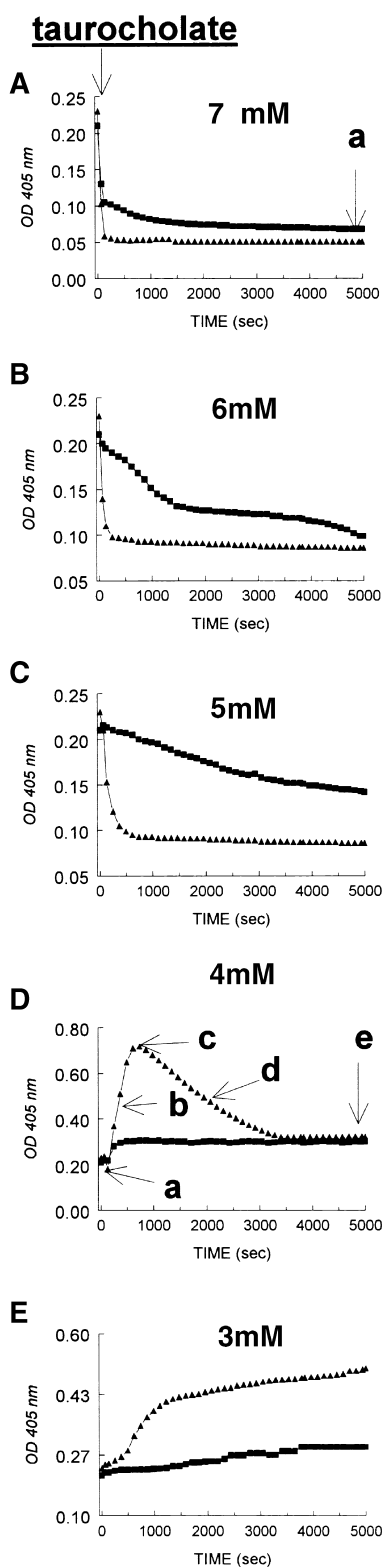


**Fig. 1.** Effects of taurocholate on sonicated small unilamellar vesicles without cholesterol, composed with 100% phosphatidylcholine (PC) or with 40% of PC replaced by sphingomyelin (SM) (final phospholipid concentration 4 mM, 37°C). As shown by the decrease of absorbance values (OD 405 nm), in case of excess taurocholate, vesicles exhibit enhanced sensitivity to detergent when SM is also included in the bilayer. (final taurocholate concentration 7 mM, 6 mM, and 5 mM; A, B and C, respectively). At lower taurocholate concentrations (4 mM in D; 3 mM in E) an increase of the absorbance values can be observed. (each time point represents mean of eight experiments. SEMs are contained within the symbols). Square, EYPC; triangle, EYSM.

This system was recently developed in collaboration with one of the authors (Frederik) based on the work by Bellare et al. (27) and Frederik et al. (28). Within an environmental chamber (temperature controlled and equipped with an ultrasonic device generating a mist to attain a relative humidity of  $\sim 100\%$ ), a specimen grid is dipped into a suspension, withdrawn, and excess liquid is blotted away between two filter papers backed by foam pads. Thin films are formed between the bars of the grid and, to vitrify these thin films, the grid is shot into melting ethane placed just outside the chamber and accessed through a shutter. Once a thin film is formed, it has a large surface to volume ratio, which makes heat and mass exchange fast processes. About dew point temperature will be attained in 0.1 s, and further evaporation may be substantial at this point. At normal room conditions (24°C, 40% relative humidity) a thin film may lose 50% of its water within 2 s and osmotic effects therefore have to be considered when not working at a 100% relative humidity (see also Hubert et al. and Frederik et al., Conference proceedings EUREM Brno 2000) (29). Therefore, all experiments in the present study are conducted at 37°C with 100% relative humidity.

When the vitrification robot is set up (vial with suspension in place, filter papers mounted, all parameters set) a forceps with grid is loaded from outside and melting ethane is prepared and for the rest the preparation/vitrification process runs automatically under PC command to end with a grid in melting ethane. The grids with vitrified thin films were analyzed in a CM-12 transmission microscope (Philips, Eindhoven, The Netherlands) at  $-170^\circ\text{C}$  using a Gatan-626 cryo-specimen holder and cryo-transfer system (Gatan, Warrendale, PA). The vitrified films were studied at 120 kV with a pressure lower than  $0.2 \times 10^{-3}$  Pa, and, at standard low-dose conditions, micrographs were taken.

## RESULTS

### Resistance of phospholipid vesicles against detergent bile salts in the absence of cholesterol

As shown in **Fig. 1A–C**, vesicles without cholesterol and containing PC as the sole phospholipid tended to be rather resistant against the detergent effects of taurocholate, as indicated by the relatively slow decrease of absorbance values during the time period studied (conditions: vesicular phospholipid 4 mM final concentration, addition of taurocholate at 7–5 mM final concentration, 37°C). Partial replacement of vesicular PC by SM, without inclusion of cholesterol, led to significant vesicular destabilization, as evidenced by low absorbance values upon addition of taurocholate. Figure 1D–E show the results obtained upon incubation of the same vesicle population with progressively decreasing concentrations of taurocholate. At taurocholate concentration of 4 mM (**Fig. 1D**) added to PC-containing vesicles, a small increase of the absorbance can be observed. In case of SM-PC vesicles, there is a large but transient increase of absorbance after addition of 4 mM taurocholate. After addition of taurocholate at a concentration of 3 mM (**Fig. 1E**), increased absorbance persists during the experiment, especially in case of SM-PC vesicles.

In **Fig. 2**, the time-course of SM-PC vesicle  $\rightarrow$  micelle transitions after addition of equimolar (4 mM) taurocholate is visualized by sequential cryotransmission electron microscopy (TEM). Initial vesicles before addition of the detergent are spherical (**Fig. 2A** and time point a in **Fig.**

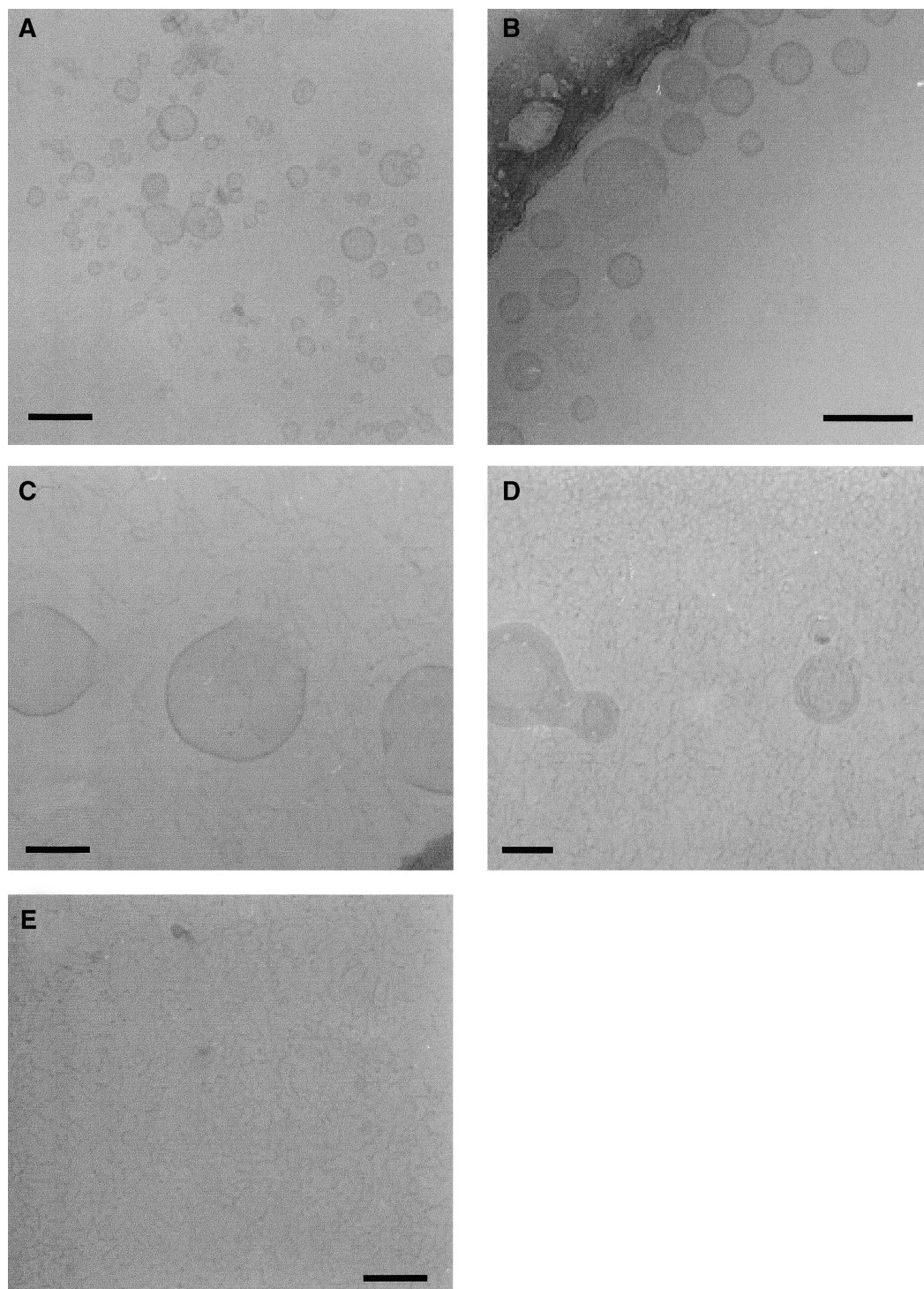


**Fig. 2.** Cryo-transmission electron microscopic images after addition of equimolar taurocholate (4 mM final concentration) to sonicated small unilamellar vesicles composed with 40% SM and 60% PC without cholesterol (final phospholipid concentration 4 mM, preparation at 37°C, 100% relative humidity). A: Sphere-like vesicles (max size ~60 nm) at initiation of the experiment (time point a in Fig. 1D). B: During the uphill part of the absorbance curve (time point b in Fig. 1D), there are some open vesicles (max size ~100 nm). C: At the absorbance peak (time point c in Fig. 1D), progressive fusion of open vesicles has resulted in large open structures, about 200 nm in diameter, coexisting with thread-like micelles. D: At the absorbance peak (time point c in Fig. 1D), some multilamellar and fused vesicular structures are also present, together with thread-like micelles. E: At the end of experiment, there are large numbers of thread-like micelles (time point e in Fig. 1D). Bar represents 100 nm.

1D). During the uphill part of the absorbance curve (time point b in Fig. 1D), multiple small vesicles coexist with some open vesicles with larger diameters. Maximal vesicular sizes have increased from 60 nm to 100 nm diameter (Fig. 2B). At the absorbance peak (time point c in Fig. 1D), progressive fusion of open vesicles results in large open structures, about 200 nm in diameter, coexisting with thread-like micelles. These large open structures have a surface area that is about 30 times the area of a small unilamellar vesicle in the starting suspension (Fig. 2C). At the absorbance peak, some multilamellar and fused vesicles are also present (Fig. 2D). During the downhill part of the absorbance curve (time point d in Fig. 1D; results not shown) and at the end of the experiment (time point e in Fig. 1D), a uniform picture of long thread-like micelles is present (Fig. 2E). In contrast, cryo-TEM after addition of excess (7 mM) taurocholate to SM-PC vesicles revealed globular micelles at the end of the experiment (time point a in Fig. 1A; results not shown).

### Resistance of cholesterol-containing phospholipid vesicles against detergent bile salts

As shown in Fig. 3A, incorporation of cholesterol in SM-PC vesicles prevents the destabilizing effect of SM (conditions: vesicular phospholipid 4 mM final concentration; vesicular SM/PC 40%/60%; vesicular cholesterol/phospholipid ratio 0.4; addition of taurocholate at 7 mM final concentration; 37°C). Absorbances of these cholesterol-enriched vesicles were stable in case of PC as the sole vesicular phospholipid, but increased markedly in the case of incorporation of SM in the vesicles. The same happened with incubation at lower taurocholate concentrations (6 mM, 5 mM, 4 mM, and 3 mM; Fig. 2B, C, D, and E, respectively).

In Fig. 4, the time-course of phase transitions after addition of 4 mM taurocholate to cholesterol-containing SM-PC vesicles is followed by sequential cryo-TEM. As shown in Fig. 4A, initial vesicles often appear ellipsoid (time point a in Fig. 3D). During the uphill part of the absorbance curve (time point b in Fig. 3D), large numbers of multilamellar vesicles are observed, together with disk-like micelles (Fig. 4B). At the end of the experiments (time point c in Fig. 3D), extremely large vesicular structures are present (Fig. 4C). Concomitant light microscopy revealed numerous aggregated and fused large vesicular structures.

## DISCUSSION

The present study points to a key role of cholesterol in formation of pathophysiologically relevant PC plus SM-containing bilayers and in modulating interactions between those vesicles and detergent bile salts. We have visualized a time-course of bile salt-induced phase transitions with the aid of state-of-the-art cryo-TEM. By vitrification from 37°C with 100% relative humidity, osmotic and temperature-induced artifacts are prevented, thus allowing

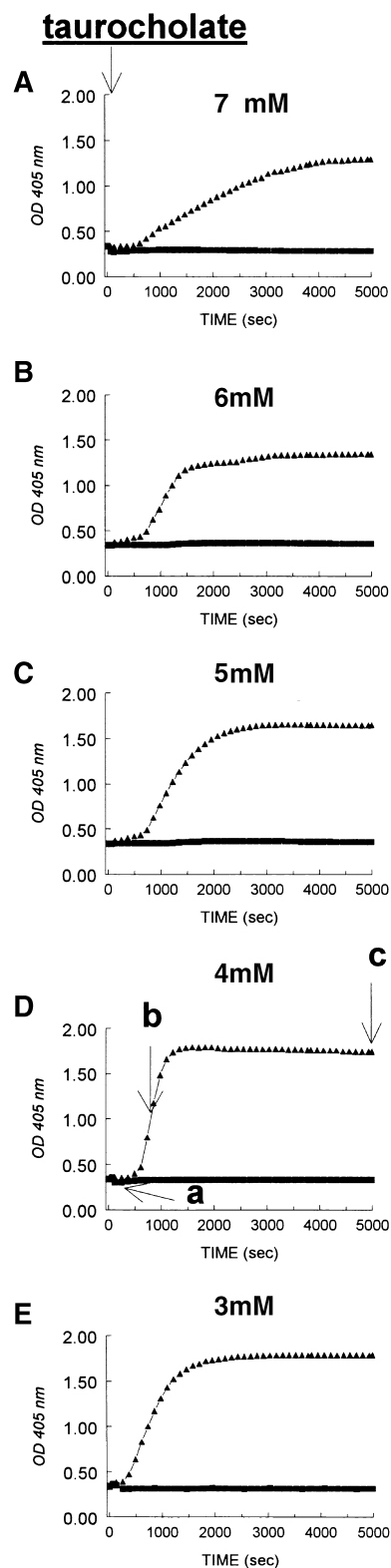


**Fig. 3.** Effects of taurocholate on sonicated small unilamellar vesicles composed with fixed amounts of cholesterol (cholesterol-PL ratio = 0.4) and with 100% PC or with 40% of PC replaced by SM (final phospholipid concentration 4 mM, 37°C). Incorporation of cholesterol prevents the destabilizing effects of SM (taurocholate final concentration 7 mM in A; 6 mM in B; 5 mM in C; 4 mM in D; 3 mM in E). (Each time point represents mean of eight experiments. SEMs are contained within the symbols). Square, EYPC; triangle, EYSM.

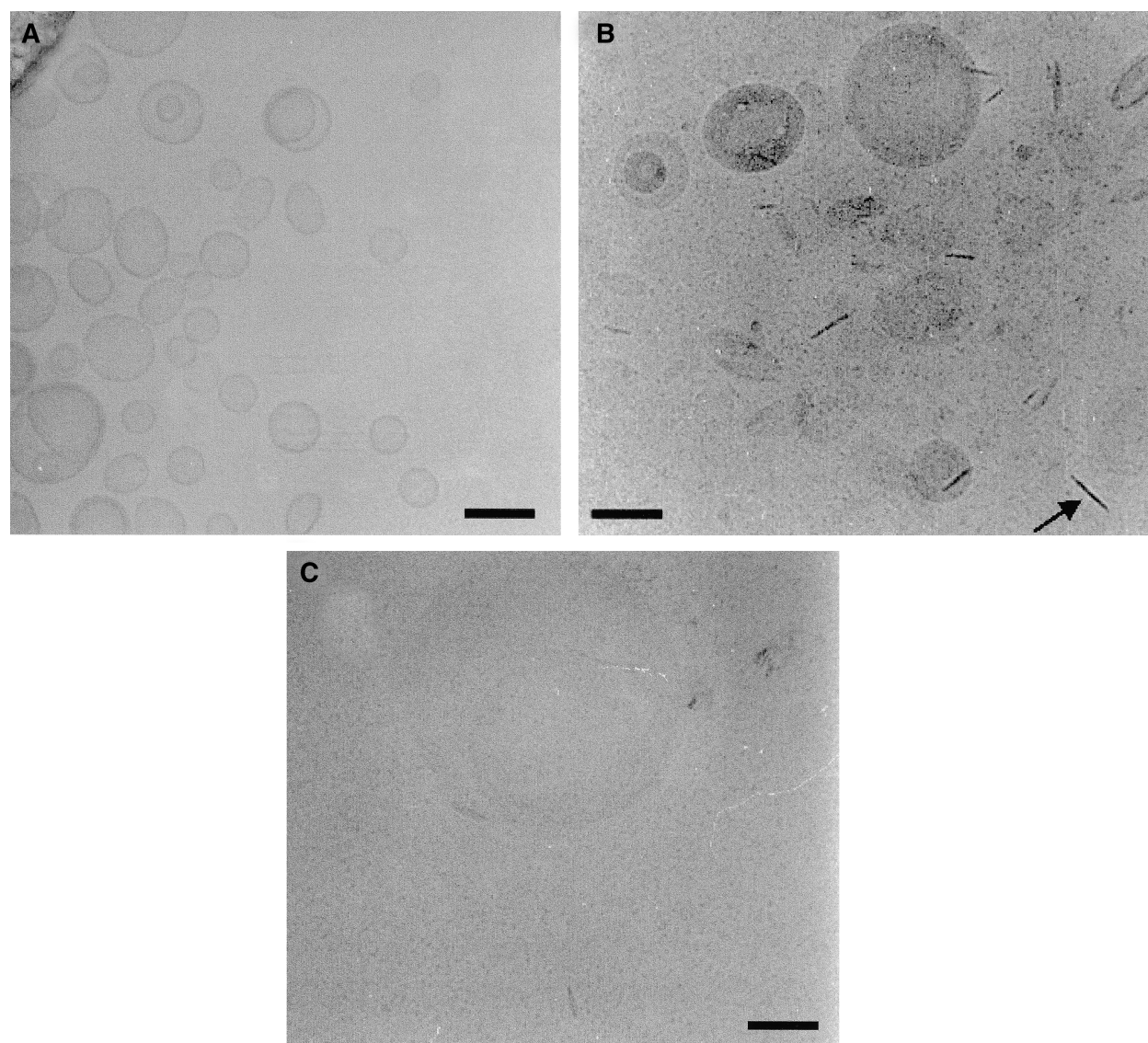


**Fig. 4.** Cryo-transmission electron microscopy images after addition of taurocholate (4 mM final concentration) to sonicated small unilamellar SM/PC vesicles (final phospholipid concentration 4 mM, SM-PC ratio 40:60, cholesterol-phospholipid ratio 0.4, 37°C, 100% humidity). A: Some vesicles have an ellipsoid shape at the initiation of the experiment (time point a in Fig. 3D). B: During the uphill part of the absorbance curve (time point b in Fig. 3D), large numbers of multilamellar vesicles are observed, together with disk-like micelles (arrow). C: At the end of the experiment (time point c in Fig. 3D), extremely large vesicular structures are present. Bar represents 100 nm.

observation of lipid-rich structures close to their original state. At the moment of vitrification by ultra-rapid cooling ( $10^{-5}$  s), the vapor pressure reduces, and all supramolecular motions are arrested, thereby preserving microstructures and avoiding any artifacts related to crystallization of water and other compounds (27–29).

Previous studies have examined in detail phase transitions induced by the addition of detergent to egg yolk PC-containing vesicles or by dilution of micellar solutions, with formation of long cylindrical micelles as intermediate structures (10, 11, 30, 31). In the present study, we have focused on phase transitions of SM-PC vesicles, with or without cholesterol incorporated in the bilayer, after addition of various amounts of taurocholate. In the absence of cholesterol, and after addition of molar excess taurocholate (final taurocholate-phospholipid ratio  $>1$ ), the bi-

layer was apparently solubilized in subunits of progressively decreasing sizes (see OD readings in Fig. 1A–C). Under these circumstances, SM-containing vesicles exhibited increased sensitivity to the detergent, compared with vesicles composed exclusively with EYPC, with the result that less time elapsed before equilibrium was reached (Fig. 1A–C). These data are in line with previous reports (32–34). Interactions between 6 mM taurocholate and 4 mM SM-PC vesicles induced slower micellization of those vesicles than 7 mM taurocholate, and there is a suggestion of biphasic solubilization (Fig. 1B). The same applies to a lesser extent for 5 mM taurocholate (Fig. 1C). We believe that the end point of these curves is complete micellization. However, we cannot exclude the possibility that a few transient open bilayers and bilayer fragments could be formed, thereby inducing biphasic solubilization curves.

At equimolar taurocholate-phospholipid ratios there was a strong but transient increase of absorbance values. Sequential cryo-TEM revealed open vesicles in the early stages after addition of the detergent. Under equimolar conditions, these open vesicles apparently have life times and density in solution that allow them to mutually interact and fuse into larger entities. As a result, large open structures together with some multilamellar and fused vesicles are visualized at the absorbance peak. Finally (coinciding with low absorption values), there is a uniform picture of thread-like micelles. Open vesicular structures that we visualized in the early stages after addition of the detergent have been described before (6) and may indicate initiation of transition toward micellar phases. Upon addition of low amounts of taurocholate (taurocholate-phospholipid ratio  $<1$ ), increased absorbance values persisted during the experiment, indicating that amounts of taurocholate were apparently not sufficient to induce the final step of complete dissociation into micelles (Fig. 1E). After addition of excess taurocholate (taurocholate-phospholipid ratio  $>1$ ), the resulting bile salt-phospholipid mixtures plot in the one-phase zone (only micelles) of the equilibrium ternary phase diagram (35, 36) and vesicle  $\rightarrow$  micelle transitions progress at extremely fast rates, thus precluding visualization of potential intermediate structures. In contrast, after addition of equimolar amounts of taurocholate (taurocholate-phospholipid ratio  $=1$ ), resulting model systems plot near or at the border of the one-phase (micellar) zone and the right two-phase (micelles and vesicles-containing) zone (35, 36), and vesicle  $\rightarrow$  micelle transitions progress at slow rates, thus allowing visualization of intermediate structures.

Incorporation of cholesterol in the vesicular bilayer had profound effects on detergent-induced phase transitions. In the absence of the sterol, and in the earliest stages, spherical vesicles were visualized, but in the presence of the sterol the vesicles often had an ellipsoid shape (Fig. 2A vs. 4A). The changes in bilayer two-dimensional conformation observed in the presence of cholesterol may be due to interactions between aliphatic chains of two sterol molecules (one in each membrane leaflet) in cholesterol-SM microdomains (37), thus inducing a local decrease in bilayer curvature. Interestingly, Crawford et al. (1, 38), with the aid of electron microscopy, could visualize in the bile canaliculi mostly ellipsoid non-spherical unilamellar vesicles, which probably contained cholesterol and phospholipid. It has been postulated that the non-spherical shapes of vesicles with decreased curvatures at the lateral sides may have relevance for interactions of cholesterol with detergent bile salts and subsequent solubilization in mixed micelles (38).

SM-PC vesicles with cholesterol incorporated in the bilayers were highly resistant against detergent-induced micellar solubilization. Intermediate multilamellar vesicles, disk-like micelles, and (at the end of the experiments) large vesicular aggregates were formed upon addition of the detergent. SM exhibits a much higher gel to liquid crystalline phase transition temperature ( $T_m$ ) than egg yolk PC: whereas egg yolk PC has a  $T_m$  below  $0^\circ\text{C}$  (39), we

previously found  $T_m$  of hydrated egg yolk SM to be  $36.6^\circ\text{C}$  (34). Pure phospholipids exist in a solid, ordered gel phase below a melting temperature ( $T_m$ ) that is characteristic of each lipid, and in a liquid disordered (also called liquid crystalline) phase above  $T_m$ .  $T_m$  of egg yolk SM is close to the incubation temperature in our experiments including preparation for cryo-EM. For this lipid species it is therefore particularly essential to attain 100% humidity (as in the present study) during cryo-preparation to prevent a temperature drop (dew-point effect) below  $T_m$ , which is known to change the shape of vesicles. The phase behavior around  $T_m$  is influenced by presence of cholesterol; lipids with a high  $T_m$  in the pure state (e.g., disaturated PC species and sphingomyelins) may form a so called liquid-ordered phase around  $T_m$  (40–42). This liquid-ordered phase has properties intermediate between the gel and liquid-crystalline phases. Like in the gel phase, tight acyl-chain packing and relatively extended acyl chains characterize the liquid-ordered phase. On the other hand, like lipids in the liquid-crystalline phase, lipids in the liquid-ordered phase exhibit relatively rapid lateral mobility within the bilayer. Recent data indicate that in bilayers containing more than one phospholipid, in the presence of cholesterol, phase separation of the phospholipids with the higher  $T_m$  (such as SM) into cholesterol-rich liquid-ordered domains occurs, and that such a phase separation is a prerequisite for detergent-resistance (41, 42). We propose that, when present together with cholesterol in liquid ordered domains, SM becomes relatively resistant to the micellizing effects of detergent bile salts. Therefore, reduced intestinal cholesterol absorption by dietary SM enrichment (20, 21) may be attributed to reduced micellization of cholesterol-SM bilayers by intestinal bile salts.

In conclusion, we have shown that incorporation of sphingomyelin in egg yolk phosphatidylcholine vesicles enhances vesicle  $\rightarrow$  micelle phase transitions, with intermediate formation of intermediate large, open, multilamellar, and fused vesicular structures. When cholesterol is also included in the bilayer, sphingomyelin-egg yolk phosphatidylcholine vesicles appear resistant to bile salt-induced micellar solubilization. Instead, multilamellar and large aggregated vesicles are formed. These findings may have implications for canalicular bile formation as well as for solubilization and absorption of intestinal lipids. **FIG**

The authors wish to thank Paul Bomans (Electron Microscopy Unit, Maastricht University, The Netherlands) for his expertise on performing cryo-TEM.

## REFERENCES

1. Crawford, J. M., G. M. Mockel, A. R. Crawford, S. J. Hagen, V. C. Hatch, S. Barnes, J. J. Godleski, and M. C. Carey. 1995. Imaging biliary lipid secretion in the rat: ultrastructural evidence for vesiculation of the hepatocyte canalicular membrane. *J. Lipid Res.* **36**: 2147–2163.
2. Halpern, Z., M. A. Dudley, A. Kibe, M. P. Lynn, A. C. Breuer, and R. T. Holzbach. 1986. Rapid vesicle formation and aggregation in

- abnormal human bile. A time-lapse video enhanced contrast microscopy study. *Gastroenterology*. **90**: 875–885.
3. Kaplun, A., Y. Talmon, F. M. Konikoff, M. Rubin, A. Eitan, M. Tadmor, and D. Lichtenberg. 1994. Direct visualization of lipid aggregates in native human bile by light- and cryo-transmission electron-microscopy. *FEBS Lett.* **340**: 78–82.
  4. Konikoff, F. M., D. Danino, D. Weihs, M. Rubin, and Y. Talmon. 2000. Microstructural evolution of lipid aggregates in nucleating model and human bile visualized by cryogenic transmission electron microscopy. *Hepatology*. **31**: 261–268.
  5. Gantz, D. L., D. Q. H. Wang, M. C. Carey, and D. M. Small. 1999. Cryoelectron microscopy of a nucleating model bile in vitreous ice: formation of primordial vesicles. *Biophys. J.* **76**: 1436–1451.
  6. Callisen, T. H., and Y. Talmon. 1998. Direct imaging by cryo-TEM shows membrane break-up by phospholipase A2 enzymatic activity. *Biochemistry*. **37**: 10987–10993.
  7. Almog, S., T. Kushnir, S. Nir, and D. Lichtenberg. 1986. Kinetic and structural aspects of reconstitution of phosphatidylcholine vesicles by dilution of phosphatidylcholine-sodium cholate mixed micelles. *Biochemistry*. **25**: 2597–2605.
  8. Lichtenberg, D., Y. Zilberman, P. Greenzaid, and S. Zamir. 1979. Structural and kinetic studies on the solubilization of lecithin by sodium deoxycholate. *Biochemistry*. **18**: 3517–3525.
  9. Almog, S., B. J. Litman, W. Wimley, J. Cohen, E. J. Wachtel, Y. Barenholz, A. Ben-Shaul, and D. Lichtenberg. 1990. States of aggregation and phase transformations in mixtures of phosphatidylcholine and octyl glucoside. *Biochemistry*. **29**: 4582–4592.
  10. Walter, A., P. K. Vinson, A. Kaplun, Y. Talmon, and Z. R. Vlahcevic. 1991. Intermediate structures in the cholate-phosphatidylcholine vesicle-micelle transition. *Biophys. J.* **60**: 1315–1325.
  11. Vinson, P. K., Y. Talmon, and A. Walter. 1989. Vesicle-micelle transition of phosphatidylcholine and octyl glucoside elucidated by cryo-transmission electron microscopy. *Biophys. J.* **56**: 669–681.
  12. Hay, D. W., M. J. Cahalane, N. Timofeyeva, and M. C. Carey. 1993. Molecular species of lecithins in human gallbladder bile. *J. Lipid Res.* **34**: 759–768.
  13. Kremmer, T., M. H. Wisher, and W. H. Evans. 1976. The lipid composition of plasma membrane subfractions originating from the three major functional domains of the rat hepatocyte cell surface. *Biochim. Biophys. Acta.* **455**: 655–664.
  14. Lund-Katz, S., H. M. Laboda, L. R. McLean, and M. C. Phillips. 1988. Influence of molecular packing and phospholipid type on rates of cholesterol exchange. *Biochemistry*. **27**: 3416–3423.
  15. Bar, L. K., Y. Barenholz, and T. E. Thompson. 1987. Dependence on phospholipid composition of the fraction of cholesterol undergoing spontaneous exchange between small unilamellar vesicles. *Biochemistry*. **26**: 5460–5465.
  16. Mattjus, P., R. Bittman, C. Vilcheze, and J. P. Slotte. 1995. Lateral domain formation in cholesterol/phospholipid monolayers as affected by the sterol side chain conformation. *Biochim. Biophys. Acta.* **1240**: 237–247.
  17. Schroeder, R. J., E. London, and D. A. Brown. 1994. Interactions between saturated acyl chains confer detergent resistance on lipids and glycosylphosphatidylinositol (GPI)-anchored proteins: GPI-anchored proteins in liposomes and cells show similar behavior. *Proc. Natl. Acad. Sci. USA.* **91**: 12130–12134.
  18. Parodi, P. W. 1997. Cows' milk fat components as potential anticarcinogenic agents. *J. Nutr.* **127**: 1055–1060.
  19. Nyberg, L., A. Nilsson, P. Lundgren, and R. D. Duan. 1997. Localization and capacity of sphingomyelin digestion in the rat intestinal tract. *J. Nutr. Biochem.* **8**: 112–118.
  20. Nyberg, L., R. Duan, and A. Nilsson. 2000. A mutual inhibitory effect on absorption of sphingomyelin and cholesterol. *J. Nutr. Biochem.* **11**: 244–249.
  21. Eckhardt, E. R. M., D. Q. Wang, J. M. Donovan, and M. C. Carey. 2002. Dietary sphingomyelin suppresses intestinal cholesterol absorption by decreasing thermodynamic activity of cholesterol monomers. *Gastroenterology*. **122**: 948–956.
  22. Yao, L., J. E. Heubi, D. D. Buckley, H. Fierra, K. D. Setchell, N. A. Granholm, P. Tso, D. Y. Hui, and L. A. Woollett. 2002. Separation of micelles and vesicles within luminal aspirates from healthy humans. Solubilization of cholesterol after a meal. *J. Lipid Res.* **43**: 654–660.
  23. Hakomori, S. 1983. Chemistry of glycosphingolipids. In *Handbook of Lipid Research*. D. J. Hanahan, editor. New York, Plenum Press. 37–39.
  24. Turley, S. D., and J. M. Dietschy. 1978. Reevaluation of the  $3\alpha$ -hydroxysteroid dehydrogenase assay for total bile acids in bile. *J. Lipid Res.* **19**: 924–928.
  25. Rouser, G., S. Fleischer, and A. Yamamoto. 1970. Two dimensional thin layer chromatographic separation of polar lipids and determination of phospholipids by phosphorus analysis of spots. *Lipids*. **5**: 494–496.
  26. Fromm, H., P. Hamin, H. Klein, and I. Kupke. 1980. Use of a simple enzymatic assay for cholesterol analysis in human bile. *J. Lipid Res.* **21**: 259–261.
  27. Bellare, J. R., H. T. Davis, L. E. Scriven, and Y. Talmon. 1988. Controlled environment vitrification system: an improved sample preparation technique. *J. Electron Microsc. Tech.* **10**: 87–111.
  28. Frederik, P. M., M. C. Stuart, P. H. Bomans, W. M. Busing, K. N. Burger, and A. J. Verkleij. 1991. Perspective and limitations of cryo-electron microscopy. From model systems to biological specimens. *J. Microsc.* **161**: 253–262.
  29. Burger, K. N., R. W. Staffhorst, H. C. de Vrijlder, M. J. Velinova, P. H. Bomans, P. M. Frederik, and B. de Kruijff. 2002. Nanocapsules: lipid-coated aggregates of cisplatin with high cytotoxicity. *Nat. Med.* **8**: 81–84.
  30. Long, M. A., E. W. Kaler, and S. P. Lee. 1994. Structural characterization of the micelle-vesicle transition in lecithin-bile salt solutions. *Biophys. J.* **67**: 1733–1742.
  31. Cohen, D. E., G. M. Thurston, R. A. Chamberlin, G. B. Benedek, and M. C. Carey. 1998. Laser light scattering evidence for a common wormlike growth structure of mixed micelles in bile salt- and straight-chain detergent-phosphatidylcholine aqueous systems: relevance to the micellar structure of bile. *Biochemistry*. **37**: 14798–14814.
  32. Schubert, R., and K-H. Schmidt. 1988. Structural changes in vesicle membranes and mixed micelles of various lipid compositions after binding of different bile salts. *Biochemistry*. **27**: 8787–8794.
  33. Moschetta, A., G. P. vanBerge-Henegouwen, P. Portincasa, G. Palasciano, A. K. Groen, and K. J. van Erpecum. 2000. Sphingomyelin exhibits greatly enhanced protection compared with egg yolk phosphatidylcholine against detergent bile salts. *J. Lipid Res.* **41**: 916–924.
  34. Eckhardt, E. R. M., A. Moschetta, W. Renooij, S. S. Goerdalay, G. P. vanBerge-Henegouwen, and K. J. van Erpecum. 1999. Asymmetric distribution of phosphatidylcholine and sphingomyelin between micellar and vesicular phases: potential implication for canalicular bile formation. *J. Lipid Res.* **40**: 2022–2033.
  35. Wang, D. Q. H., and M. C. Carey. 1996. Complete mapping of crystallization pathways during cholesterol precipitation from model bile: influence of physical-chemical variables of pathophysiologic relevance and identification of a stable liquid crystalline state in cold, dilute and hydrophilic bile salt-containing systems. *J. Lipid Res.* **37**: 606–630.
  36. van Erpecum, K. J., and M. C. Carey. 1997. Influence of bile salts on molecular interactions between sphingomyelin and cholesterol: relevance to bile formation and stability. *Biochim. Biophys. Acta.* **1345**: 269–282.
  37. Sankaram, M. B., and T. E. Thompson. 1991. Cholesterol-induced fluid-phase immiscibility in membranes. *Proc. Natl. Acad. Sci. USA.* **88**: 8686–8690.
  38. Crawford, A. R., A. J. Smith, V. C. Hatch, R. P. J. Oude Elferink, P. Borst, and J. M. Crawford. 1997. Hepatic secretion of phospholipid vesicles in the mouse critically depends on mdr2 or MDR3 P-glycoprotein expression. Visualization by electron microscopy. *J. Clin. Invest.* **100**: 2562–2567.
  39. Koynova, R., and M. Caffrey. 1995. Phases and phase transitions of the sphingolipids. *Biochim. Biophys. Acta.* **1255**: 213–236.
  40. Xiang, T. X., and B. D. Anderson. 1998. Phase structures of binary lipid bilayers as revealed by permeability of small molecules. *Biochim. Biophys. Acta.* **1370**: 64–76.
  41. Ahmed, S. N., D. A. Brown, and E. London. 1997. On the origin of sphingolipid/cholesterol-rich detergent-insoluble cell membranes: physiological concentrations of cholesterol and sphingolipid induce formation of a detergent-insoluble, liquid-ordered lipid phase in model membranes. *Biochemistry*. **36**: 10944–10953.
  42. Schroeder, R. J., S. N. Ahmed, Y. Zhu, E. London, and D. A. Brown. 1998. Cholesterol and sphingolipid enhance the triton X-100 insolubility of glycosylphosphatidylinositol-anchored proteins by promoting the formation of detergent-insoluble ordered membrane domains. *J. Biol. Chem.* **273**: 1150–1157.